



Investigation of the manufacturability of a copper coil for use in space components by means of the fused filament fabrication process

S. Uffelmann¹ · S. Pestotnik²

Received: 28 February 2022 / Revised: 25 September 2022 / Accepted: 4 October 2022 / Published online: 15 October 2022
© The Author(s) 2022

Abstract

Metal-filled polymers can serve as the starting material to produce complex metal structures using the cost-effective additive manufacturing process Fused Filament Fabrication (FFF). In this process, the filaments consisting of polymer binders (e.g., polylactic acid (PLA)) and micropowder of highly conductive metals (e.g., copper) are extruded through a nozzle to build up the desired geometry layer by layer. The manufacturability of a complex copper coil for use in satellite actuators with two commercially available filaments (Electrifi and Filamet Copper) using FFF was investigated and the electrical conductivity of the printed material was determined. A design of experiment with variation of extruder temperature and printing speed was used to evaluate different parameter sets. The selected parameter set was then used to produce cuboids to determine the electrical conductivity and an exemplary coil geometry. While the coil could be printed in two sizes (original and enlarged by a factor of two) with one of the investigated filaments, this was not possible with the other filament because the printed material was not dimensionally stable with the selected process parameter set. For the Electrifi filament, that is electrically conductive without post processing, the material achieved a maximum electrical conductivity of $5.59 \cdot 10^{-3}$ % IACS ($0.033 \Omega\text{cm}$). This was in alignment with other published results for this filament. The other filament Filamet Copper is not conductive in the as-built state. After debinding and sintering, the material achieved a maximum electrical conductivity of 45.84% IACS ($3.77 \cdot 10^{-6} \Omega\text{cm}$).

Keywords Additive manufacturing · Fused filament fabrication · Copper · Electrical conductivity · Electromagnetic space components · Magnetic bearing coil

1 Introduction

In spaceflight, the drive to make all components smaller and lighter is more present than ever. The development of CubeSats has played a significant part in this trend. For this reason, many researchers are working on reducing the size of satellite components.

Additive manufacturing (AM) can be seen as one option to produce topology optimized lightweight structures. AM has therefore become a focus area for many industrial users in recent years. AM forms a family of different processes that have been grouped together in recent years by the

American Society for Testing and Materials (ASTM) and the International Organization for Standardization (ISO), among others. In general, AM processes are characterized by the possibility of producing components with increased complexity compared to conventional manufacturing processes such as turning and milling. For the user, the question arises as to which of the additive processes is best suited for their own application. In the space industry, work on the application of additively manufactured copper has been conducted at the Marshall Space Flight Center as part of NASA's Low-Cost Upper Stage Propulsion Program. Both rocket liners and combustors have been successfully developed and hot-fired [1–8].

Satellite components supplier ZARM Technik AG developed customized electromagnetic coils with a complex geometry for space actuators, initially from aluminum. To increase the electrical conductivity of these coils, they are now being developed using copper instead of aluminum. The study of this work is part of the benchmark, conducted as

✉ S. Uffelmann
suffelmann@stud.hs-bremen.de

¹ City University of Applied Sciences Bremen, Bremen, Germany

² ZARM Technik AG, Bremen, Germany

part of this development project, which compares different additive manufacturing (AM) processes.

The study presented in this paper focuses on the production planning and implementation of additively manufactured coils made of copper using Fused Filament Fabrication (FFF). The objective is to manufacture a complex coil geometry and investigate the electrical conductivity of the material produced using this process with state-of-the-art AM equipment. Another objective is to determine whether the electrical conductivity reported in publications can be verified with FFF-processed copper material produced in this study. Literature research is carried out to identify potential process parameters and suitable test print geometries to be investigated. The most suitable process parameters for each of the investigated filaments are determined using a Design of Experiment (DoE). Cuboids and coils are printed with the selected parameter sets and evaluated through visual inspection and geometric accuracy measurement. The printed material is additionally examined with regard to its electrical conductivity. The results are compared with values reported in the literature.

2 State-of-the-art

Although the FFF process was developed in the 1980s, printing with metal filaments has only been possible for a few years [9]. Printing with various plastic filaments still occupies a central place in research. However, developments in recent years have brought other materials such as copper into the focus of research. Pure copper by itself cannot be processed because the FFF process works with filaments with a melting point much lower than pure copper. Therefore, copper powder is mixed with plastics to create filaments [10–13].

Since 2017, a copper filament called Electrifi, developed in 2017 by Flower et al. [14], has been of interest to researchers. Since then, numerous studies have been published on this conductive copper filament [14–22]. One theme of the publications is the comparison of the Electrifi filament with other conductive composite filaments such as Proto-Pasta (a carbon black-based conductive PLA) and Black Magic (a graphene-based conductive PLA). Flowers et al. [14] compared Electrifi with these two conductive filaments. The Electrifi filament exhibited the lowest resistance for various printed conductive traces, which was measured using current/voltage measurement. Kim et al. [18] also compared these three filaments and investigated the electrical resistances with a $0.2 \cdot 0.5 \cdot 8\text{mm}$ conductive trace. The

resistances of the printed traces were $0.025\Omega\text{cm}$ for Electrifi, $1.18\Omega\text{cm}$ for BlackMagic, and $10.83\Omega\text{cm}$ for Proto-Pasta. Colella et al. [16, 17] studied only the two filaments Electrifi and BlackMagic for antenna fabrication. The efficiency of the fully 3D-printed Electrifi-based prototype was satisfactory, although the conductive properties of the antennas fabricated with the Electrifi filament were lower than those realized with conventional fabrication techniques. The research group of Mitra et al. [19, 20] and Striker et al. [23] applied a multi-material technique for direct 3D printing of a conformal antenna based on two different filaments, the conductive Electrifi and the flexible NinjaFlex, using the FFF process. They presented a comparative study of the components of unintended near-end and far-end crosstalk between a pair of copper microstrip transmission lines in the presence of a 3D-printed conductive Electrifi trace. Two prototypes were tested for the two cases “without 3D-printed trace” and “with 3D-printed trace”. In addition, they presented a multi-material technique in which Electrifi and NinjaFlex are processed together in a single print job in a single-extruder printer. The antenna and substrate layers are thermally bonded together during the printing process without adding adhesives. Cardenas et al. [15] and Watschke et al. [22] were mainly concerned with optimizing the electrical conductivity measurement of printed Electrifi and other filament traces. Therefore, Cardenas et al. developed flash ablation metallization (FAM). Four-point resistance measurements were used to evaluate the conductivity changes for different filaments (e.g., Electrifi). Before irradiation, printed Electrifi was found to have an electrical conductivity of $2 \cdot 10^{-3}\Omega\text{cm}$. The photonicallly treated samples showed an electrical conductivity of $3 \cdot 10^{-5}\Omega\text{cm}$.

A lot of research has been done in recent years to develop conductive filaments made from copper powder and polymeric binders. The material extrusion process FFF offers a cost-effective way to additively manufacture conductive material. Advantages of the FFF process are the easy handling and storage of the filament and the availability of low-cost AM equipment [9]. Depending on the filament, subsequent post processing steps, such as debinding and sintering, are necessary. The Electrifi filament made from copper powder and PLA demonstrated its ability to produce electrically conductive material in several publications [14–22]. Especially the comparison by Flowers et al. showed that Electrifi filament produces the best electrical conductivities compared to other commercially available filaments [14]. Furthermore, the higher the copper content, the better the electrical conductivity.

Since the aim is to achieve the highest possible conductivity for the coils, Electrifi and a filament called Filamet Copper with a high copper content of 89% by mass (identified in the publication by Ebrahimi et al. [24]) were chosen. For the Electrifi filament, previous studies demonstrated that simple geometries like the cuboid and multi-material printing are possible under certain conditions. However, none of the published studies printed complex geometries. For this reason, the presented study attempts to print a complex coil geometry with the above-mentioned filaments reported in the literature. In addition, it will be investigated whether electrical conductivities similar to those found in the publications are achievable.

3 Experimental method

To investigate the manufacturability of a complex coil geometry by FFF processing, suitable parameter sets are identified using a DoE. For this purpose, test prints ($10 \cdot 10 \cdot 10$ mm · cubes) are printed using the two copper filaments under investigation. Electrifi (hereinafter: filament A) and Filamet Copper (hereinafter: filament B) are selected for this study based on the results of the literature analysis. Filament A is processed with a German RepRap $\times 400$ with two extruders with a 0.6 mm nozzle diameter (one for the filament and one for supporting structure), while filament B is processed with a CREALITY CR20 Pro with one extruder, also with a 0.6 mm nozzle diameter, due to its brittleness and thus better processability with this printer's filament feed system. Simplify 3D is used as slicer program to generate the G-code.

For the filament B a debinding and sintering process is performed at an external supplier who has experience in debinding and sintering of additively manufactured parts, mainly with binder jetted parts. The temperature distribution of the performed sintering process of parts made from filament B is shown in Fig. 1.

Surface quality (determined by visual inspection) and geometric accuracy have been selected as criteria for the

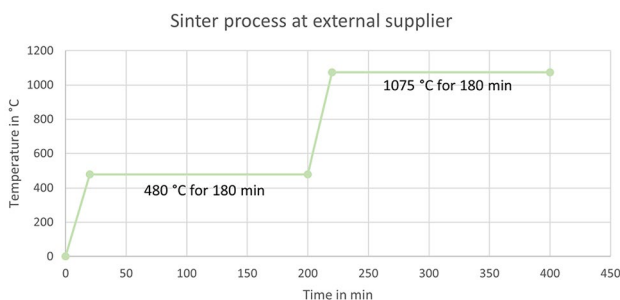


Fig. 1 Sintering process of parts made from filament B

selection of suitable process parameter sets. The surface quality is evaluated visually according to the criteria: cube is completely printed, no holes or excess material, and no scratches or dents are detected.

The geometry accuracy is measured by a calliper and passed if all dimensions are within the tolerance, which is composed of the printer tolerance (± 0.1 mm) and the general tolerance according to ISO 2768-1f.

The electrical conductivity of the FFF-processed material is determined by four-wire resistance measurements on cuboids. The measurement is carried out along the printing path along the length a (see Fig. 2) of the cuboids in the x - y plane of the printer. Clamps are attached to the ends of the cuboids for the current measurement. For the voltage measurement, a fixed spacer of 65 mm is used. The PM2831 Philips DC Power Supply is used as the current source. The voltage is measured using Agilent Technologies HP 34401A multimeter and from this the resistance is determined.

The copper content of the cuboids is analyzed using cross sections and a contrast-based image analysis. For this, a light microscope (ZEISS Axio) and the 'Olympus Stream' analysis software are utilized.

3.1 DoE for the selection of parameter sets

The DoE method is used to identify suitable parameter sets to achieve the desired printing results with the investigated filaments [13]. A more detailed description of DoE for the FFF process can be found in the literature [25–30].

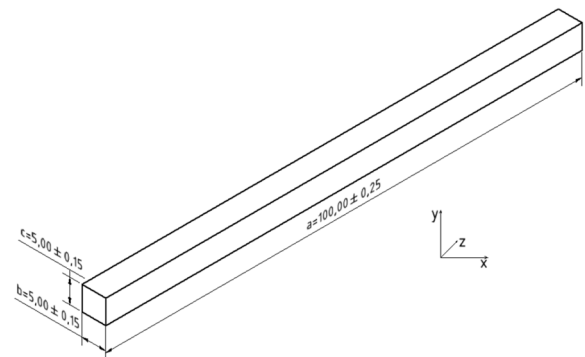
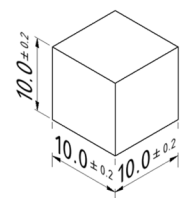


Fig. 2 Cuboids for electrical conductivity determination

Fig. 3 Cubic test print geometry



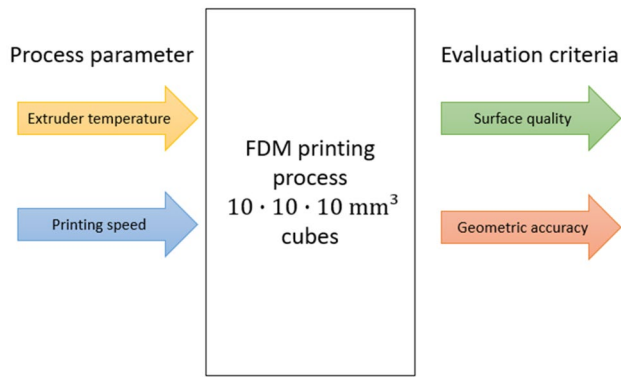


Fig. 4 Selected experimental layout for the cubic test prints

Cubic test prints (Fig. 3) are printed using various parameter sets and evaluated in terms of surface quality and geometric accuracy to select a suitable parameter set for each investigated filament.

Printing speed and extruder temperature have a significant influence on the printing result and are therefore varied in the investigation of the filaments [25, 31–34]. Other parameters, such as layer height, print bed temperature, and infill ratio also influence the printing result. Constant values are defined for these parameters, based on the recommendations of the filaments' manufacturers. The experimental layout of the cubic test prints is illustrated in Fig. 4.

Table 1 summarizes the parameters for FFF processing of filament A as recommended by the filaments' manufacturers [35–39] which are used for the printing process.

For filament A, the printing speed and extruder temperature are varied in steps of 15 mm/s and 10 °C. According to previous investigations, the extruder temperature has the greatest influence on the printing behavior [36]. It is therefore increased in smaller steps and varied first. The DoE results in a total of six parameter sets which are listed in Table 2.

For filament B, the manufacturer recommends to start the printing process at a constant speed of 30 mm/s to get an understanding of the printing behavior of the filament [39]. The layer height of 0.2 mm and the print bed temperature of 50 °C are suggested by the manufacturer and therefore adopted. After an initial variation of the extruder temperature at a printing speed of 30 mm/s, the optimal extruder temperature is kept at a constant value and the printing speed is varied in steps of 10 mm/s. A total of six different parameter sets are examined which are listed in Table 3.

Table 1 Recommended process parameters for FFF processing of the investigated filaments

	Temperature	Printing speed	Layer height	Nozzle	Infill	Print bed
FA	130–160 °C	15–45 mm/s	0.2 mm	0.6 mm	100%	Not heated
FB	205–235 °C	30–60 mm/s				50 °C

Table 2 Parameter sets investigated with filament A

Parameter set ID	Printing speed (mm/s)	Extruder temperature (°C)
FA1	15	150
FA2	30	150
FA3	45	150
FA4	45	160
FA5	45	140
FA6	45	130

Table 3 Parameter sets investigated with filament B

Parameter set ID	Printing speed (mm/s)	Extruder temperature (°C)
FB1	30	235
FB2	30	220
FB3	30	205
FB4	40	220
FB5	50	220
FB6	60	220

3.2 Cuboids and coils print planning

Cuboids (Fig. 2) are printed for electrical conductivity determination of the FFF-processed (and post processed) material using the selected parameter set for each of the two investigated filaments.

A complex coil geometry (Fig. 5) is printed to investigate whether the FFF process is suitable to produce copper electromagnetic space components. The geometry features

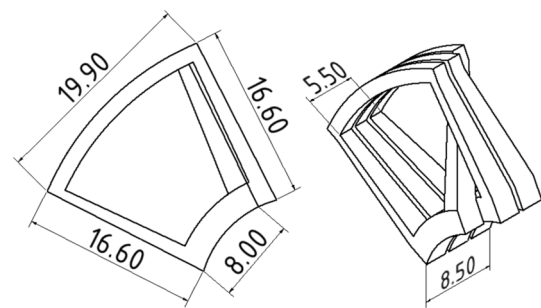


Fig. 5 Selected coil geometry for the presented study

square winding cross sections with variable cross section areas, small winding gaps, and sharp corners which are not easily manufacturable using conventional processes.

A FFF printer with two extruders is used to produce coils with filament A, as the supporting structure is printed with a commercial PLA filament using the second extruder.

Another FFF printer with only one extruder is used to produce coils with filament B. As this prevents printing supporting structure with another material, no supporting structure is used to build up coils using this filament. If filament B would be used for both the coil geometry itself and the supporting material, short-circuits would be produced after heat treatment.

The coil is printed in various orientations, i.e., 60 degree, 90 degree and side down, with and without raft, to define a suitable printing set-up. The size of the coil is scaled by a factor of two for most of the trials to facilitate the FFF processing.

4 Results

4.1 Surface quality and geometric accuracy

The selection of a suitable parameter set for FFF processing of each filament is based on the surface quality and geometric accuracy of the cubic test prints described above. Each investigated parameter set is used to print three cubes to achieve a minimal statistical relevance in the evaluation.

For filament A, the parameter study is started with a constant extruder temperature under variation of the printing speed, starting with the lowest investigated speed. The results of the test prints are shown in (Fig. 6).

Parameter set FA1 produces inferior material quality. Individual wires which are barely bonded are produced. It is not possible to achieve the targeted cube geometry. The printing process is therefore stopped prematurely.

The increase of the printing speed in parameter set FA2 generates better printing results. Nevertheless, the test prints are merely cubical and are characterized by defects and a

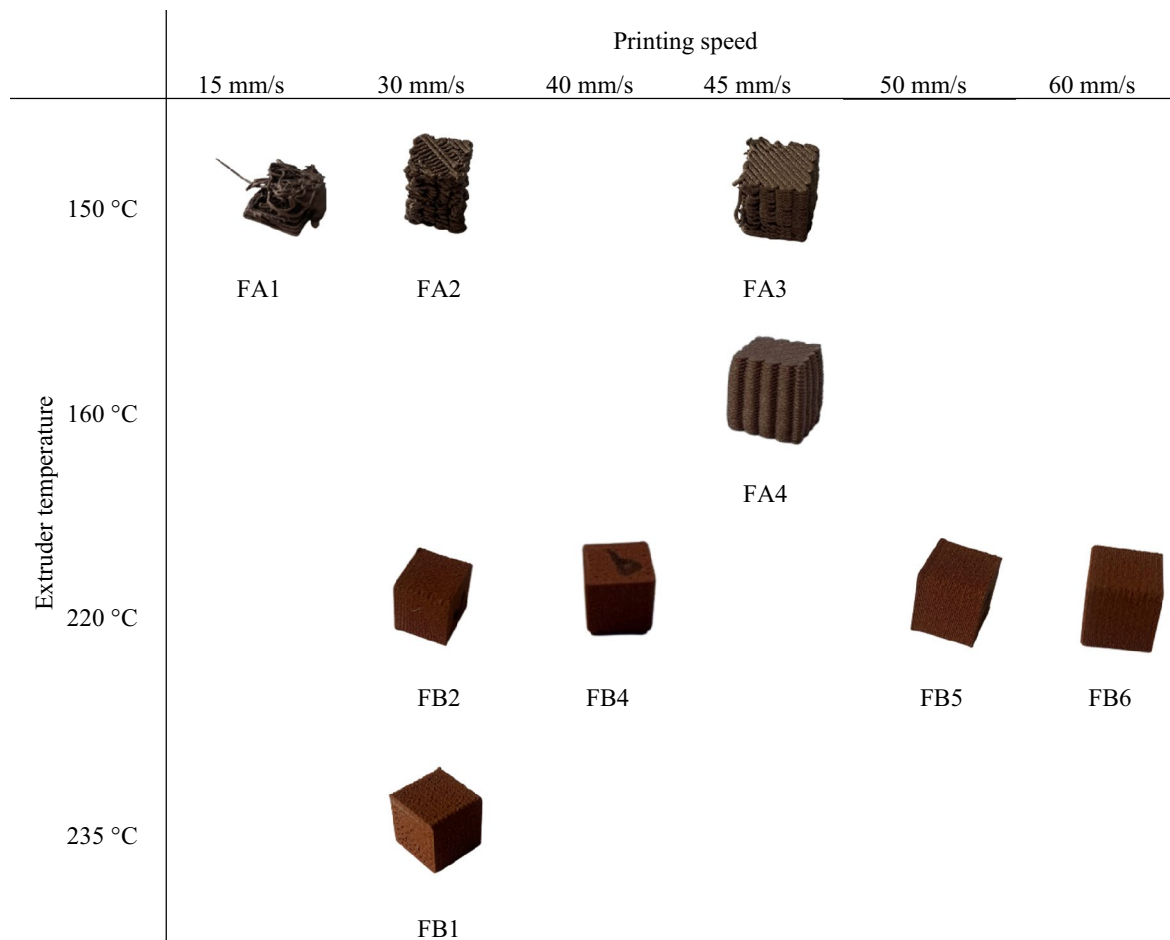


Fig. 6 Results of cubic test prints with filaments A and B

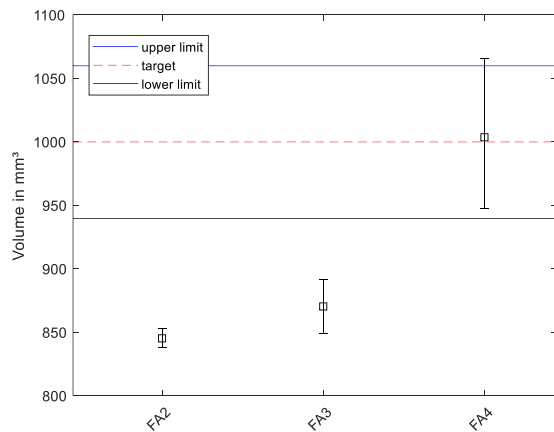


Fig. 7 Geometric accuracy of filament A based on the test print

high surface roughness. Individual layers are clearly distinguishable which suggests that the layers are not sufficiently bonded (Fig. 6). With regard to their geometric accuracy, all three cubes do not reach the targeted dimensions.

Parameter set FA3 with a printing speed of 45 mm/s achieved the best results in terms of surface quality and geometric accuracy of all parameter sets with an extruder temperature of 150 °C. Even though individual layers are still distinguishable, they are better bonded (Fig. 6). However, the width and length of the cubes are still out of tolerance.

After this initial variation of the printing speed at a constant extruder temperature, the speed is kept at 45 mm/s while the temperature is varied.

Cubic geometries with bonded layers and lower surface roughness are achieved with the increased extruder temperature of parameter set FA4. No voids or other surface defects are detected in the visual inspection and the individual dimensions are within the tolerances (except one dimension). The cube has a wavy pattern on the cube side (Fig. 6). The material is not dimensionally stable, which is why hard edges cannot be reproduced. This creates wavy patterns, which can also be seen in the cuboids, but these are

Table 4 Results of the DoE for FFF-processed filament A

Parameter set ID	Results	
	Surface quality	Geometric accuracy
FA1	×	×
FA2	×	×
FA3	✓	×
FA4	✓	×
FA5	Not printable and therefore not measured	
FA6		

more pronounced in the cubes also due to the many changes of direction due to the selected meander printing strategy.

Trials with parameter sets FA5 and FA6 reveal that FFF processing of filament A is not possible with extruder temperatures below 150 °C as material is not extruded below this threshold temperature.

Figure 7 illustrates the variation in the geometric accuracy of the test prints produced with filament A. While a volume of 1000 mm³ was targeted, the most accurate cubes processed with parameter set FA4 reach a volume of 1003.65 mm³. The material appears to not be dimensionally stable because of sagging which leads to geometric inaccuracies.

Based on the evaluation of the surface quality and geometric accuracy of the printed cubic test prints (Table 4), parameter set FA4 is selected for further FFF processing of filament A within this study. The pass criteria for the surface quality for filament A are: cubes are completely printed and have a flat top surface as seen in Fig. 8. A cube with a rough top surface is shown in the close-up image in Fig. 9.

To determine the most suitable parameter set for FFF processing of filament B, the same process parameters (but different values) are varied using a dedicated DoE. At first, a suitable extruder temperature is selected at a constant printing speed of 30 mm/s.

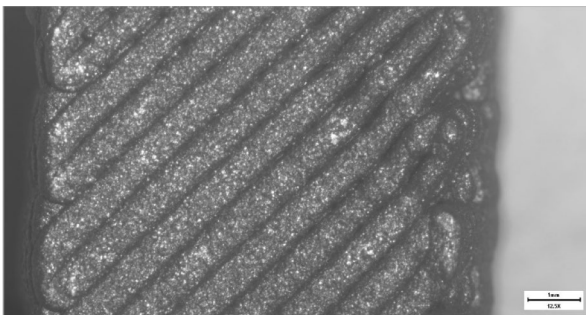


Fig. 8 Close-up image of flat top surface of cube FA4b

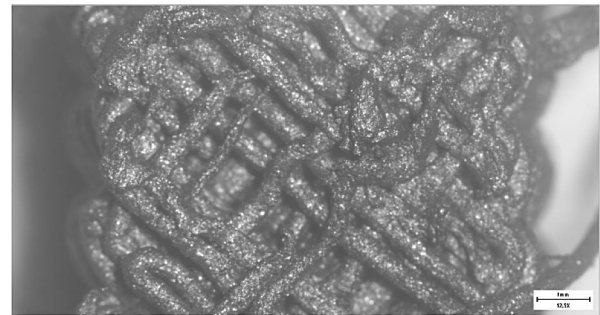


Fig. 9 Close-up image of rough top surface of cube FA2b

Parameter set FB1 with the highest investigated extruder temperature of 235 °C produces cubes whose surface looks a lot better than the ones of all cubes produced using filament A. In contrast to the subsequent parameter set FB2, the surface is rougher and the individual layers are more clearly recognizable (Fig. 6). However, the lengths of all cubes printed with this parameter set are within the tolerance limits.

Lowering the extruder temperature results in even smoother surfaces of the cubes printed with parameter set FB2 (Fig. 6). The geometric accuracy of the FB2b and FB2c cubes deviates only minimally from the target dimension. The FB2a cube can only be measured on one side in the height and width and complies with the tolerances there, but is thus excluded from the evaluation. Therefore, the parameter set FB2 passes the geometric accuracy evaluation. Since the results are promising, especially with regard to visual inspection, this is taken over into the shortlist as one of the possible parameter sets for the printing of the cuboids and the coils.

Similarly to parameter sets FA5 and FA6 of filament A, FFF processing of filament B is not possible with parameter set FB3 because no material is extruded through the nozzle below an extruder temperature of 210 °C.

After this initial variation of the extruder temperature at a constant printing speed, the temperature is kept at 220 °C while the speed is varied.

The best printing result with respect to surface quality in this DoE is achieved with parameter set FB4. Only minor pores are detected in the visual inspection which are expected to be eliminated during subsequent heat treatment steps (Fig. 6). All dimensions of the three cubes are within the tolerances.

One of the cubic test prints printed with parameter set FB5 did not adhere to the print bed and thus failed. The increased speed might be a potential reason. Two of the

cubes exceed the targeted dimensions above the defined tolerances.

Due to the high printing speed used in parameter set FB6, the individual layers do not bond as well as layers printed at lower speeds (Fig. 6). This could also be the reason why the cubes do not meet the targeted dimensions.

Figure 10 illustrates the variation in the geometric accuracy of the test prints produced with filament B. None of the test prints have a volume below the lower tolerance range of 940 mm³. However, two cubes (FB5a and FB6a) exceed the tolerance range of 1060 mm³. Cubes printed with the remaining parameter sets are within the tolerance range of the targeted volume.

Based on the evaluation of the surface quality and geometric accuracy of the printed cubic test prints (Table 5), parameter set FB4 is selected for further FFF processing of filament B within this study. As parameter set FB2 also produced cubes with good surface quality, it is additionally selected to produce cuboids for electrical conductivity assessment for comparison of the two parameter sets. The pass criteria for the surface quality for filament B are different than for filament A since the overall print result of the cubes is better. In addition to a completely printed cube and flat top surface, no excess material and no scratches or dents are pass criteria for filament B. An example for a flat top

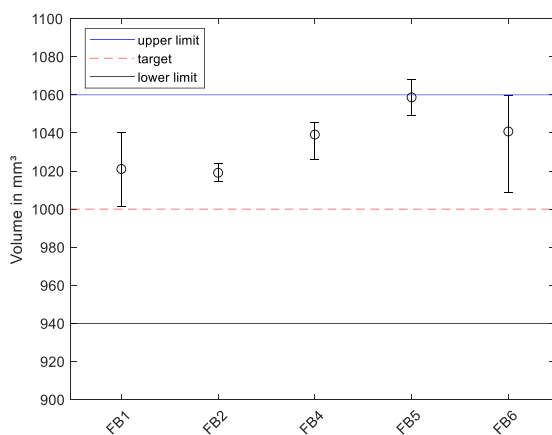


Fig. 10 Geometric accuracy of the filament B based on the test print

Table 5 Results of the printed filament B with the investigated parameter sets

Parameter set ID	Results	
	Surface quality	Geometric accuracy
FB1	✓	✓
FB2	✓	✓
FB3	Not printable and therefore not measured	
FB4	✓	✓
FB5	×	×
FB6	×	×

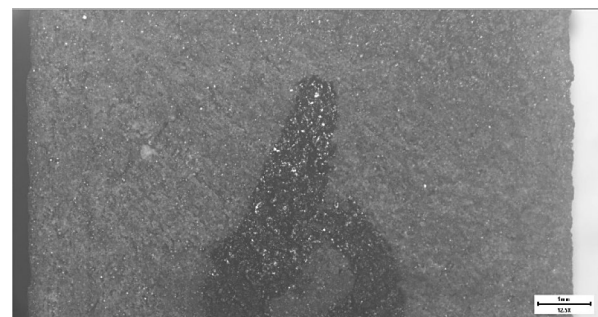


Fig. 11 Close-up image of a flat top surface of cube FB2b

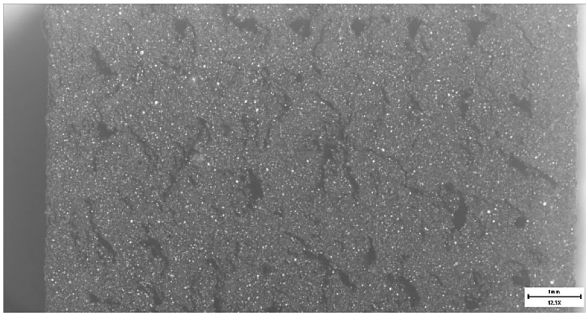


Fig. 12 Close-up image of a rough top surface of cube FB1b

surface (Fig. 11) and a rough top surface (Fig. 12) is given by a microscope close-up image of the cubes.

4.2 Electrical conductivity

Cuboids are printed for determination of the electrical conductivity of FFF-processed material of filaments A and B using the selected parameter sets FA4, FB2, and FB4.

The surfaces of cuboids (Fig. 13) made from filament A are smoother and layers are more sufficiently bonded than those of the cubic test prints printed with the same parameter set. While no distortion is observed during the printing process, both ends of the cuboid bend upwards during cool down on the print bed. A potential future countermeasure could be heating of the print bed to prevent the cuboid from cooling down too fast. Geometric accuracy measurements on the cuboids reveal that none of the cuboids achieved the targeted height and width of 5 mm. Only the length is within the tolerances for all three cuboids. It is possible that at this low height (5 mm) the distances cannot be maintained. Another reason could be that the print bed was not set correctly or that the layer thickness was assumed to be 0.2 mm, but in the end it was less.



Fig. 13 Cuboids ($5.5 \cdot 100 \text{ m}^3$) printed with process parameter FA4: **a** CubFAa, **b** CubFAB, and **c** CubFAc



Fig. 14 Cuboids ($5.5 \cdot 100 \text{ m}^3$) printed with parameter set FB2: **a** CubFB2a, **b** CubFB2b, and **c** CubFB2c

From a surface quality point of view, the cuboids printed with parameter set FB2 and FB4 with filament B, which are shown in Figs. 14, 15, are in line with the respective cubic test prints. Similarly to the cuboids printed with filament A, they do not reach the targeted height. Width and length of all cuboids exceed the targeted dimensions.

The resistance values determined by four-wire resistance measurements are converted into electrical resistivity and conductivity (expressed in comparison to the International Annealed Copper Standard; Table 6). The resistance of the filament A specified by the filament A manufacturer is 2.5Ω for an 10.9 cm long piece of filament [40]. The material produced in the reported study achieves lower resistance, and thus better conductivity of $5.37 \cdot 10^{-3} \% \text{ IACS}$ ($0.033\Omega\text{cm}$).

Cuboids printed using filament B are electrically measured before and after the heat treatment (debinding and sintering). Prior to the heat treatment, the resistance is in the range of $\text{M}\Omega$ and the material is considered non-conductive in this state like the filament itself. After the heat treatment, cuboids printed with both parameter sets achieve electrical conductivities around $45 \% \text{ IACS}$ ($3.77 \cdot 10^{-6}\Omega\text{cm}$).

4.3 Copper content

To get a better understanding of the variations in electrical conductivity of cuboids produced from both filaments, cross sections are examined with respect to the copper content of the parts.

The copper content of a cuboid printed with filament A which is electrically conductive in the as-built state without additional heat treatment steps is 23.54%. This low value



Fig. 15 Cuboids ($5.5 \cdot 100 \text{ m}^3$) printed with parameter set FB4: **a** CubFB4a, **b** CubFB4b, and **c** CubFB4c

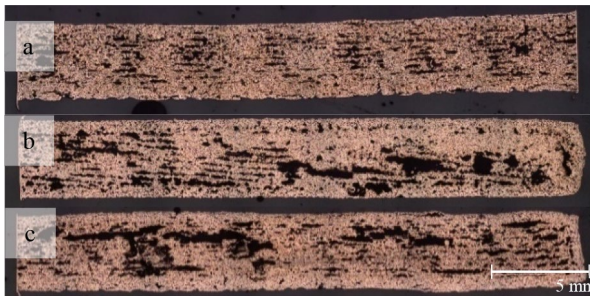
Table 6 Electrical resistance, resistivity, and conductivity of the (as-built vs. heat treated) cuboids printed with filaments A and B (in-plane measurement)

Parameter set ID	Electrical resistance	Electrical resistivity	Conductivity
CubFA4	1.64Ω	0.033Ωcm	$5.37 \cdot 10^{-3}$ % IACS
CubFB2	0.167 mΩ	$3.77 \cdot 10^{-6}$ Ωcm	45.64 % IACS
CubFB4	0.194 mΩ	$3.82 \cdot 10^{-6}$ Ωcm	45.11% IACS

explains the low conductivity. As no heat treatment is performed, the polymer binder is still present, holding together the copper particles, but also separating and thus insulating them (Fig. 16).

Cuboids printed with filament B are thermally post processed in a heat treatment consisting of debinding and sintering steps. During debinding, the polymeric binder decomposes. During the subsequent sintering, the remaining copper particles sinter together. The cross sections of cuboids printed with parameter sets FB2 (Fig. 17) and FB4 (Fig. 18) are characterized by regions of dense copper material and pores. No remains of binder are detected in the heat-treated parts. The mean copper content of the cuboid printed with parameter set FB2 is 59.33 %, while the mean copper content of the cuboid printed with parameter set FB4 is slightly lower with 58.57%. However, the dense copper regions are distributed more evenly in this cuboid.

The copper content of both cuboids is limited due to a high number of pores remaining after debinding and sintering which explains the limited electrical conductivity.

**Fig. 16** Cross-section of a cuboid printed with filament A**Fig. 17** Cross-sections **a** sub-part 1 **b** sub-part 2 **c** sub-part 3 of a cuboid printed with parameter set FB2

4.4 Complex coil geometry

Even though various orientations on the build platform are investigated, support structure made from PLA and rafts are used, and the coil geometry is enlarged by a factor of two for easier processing, it is not possible to print the coil geometry with filament A (Table 7). Similarly to the cubic test prints, individual layers are clearly distinguishable and thus not sufficiently bonded. Coils without raft do not adhere to the print bed. In addition, the extruded material is not dimensionally stable, i.e., coil windings tilt outwards. Due to this shift in the geometry, subsequent layers are not extruded on top of previous layers and the print job fails. This phenomenon is observed during each coil print trial.

Filament B is successfully used to print the targeted coil geometry in its original size (Table 8 – CoilFB3a) and enlarged by a factor of two (Table 8 – CoilFB1b) in horizontal orientation. First printing set-ups with the original parameter set FB4 are unsuccessful because the coil geometry does not adhere to the print bed with and without additional raft. An increase of the print bed temperature from 50 to 70 °C enables FFF printing of the coil geometry. Trials with and without raft show that printing of the coil directly on the print bed without raft achieves better results.

The windings of the coil show defects, such as the staircase effect on top surfaces, fringes on unsupported overhangs, voids, and holes. The small gaps between windings exist only in the enlarged coils. The windings of coils printed in the original size are fused together.

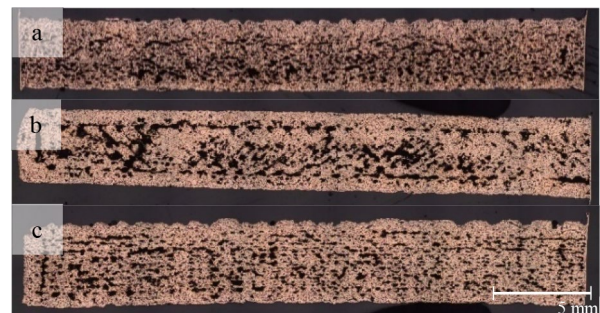
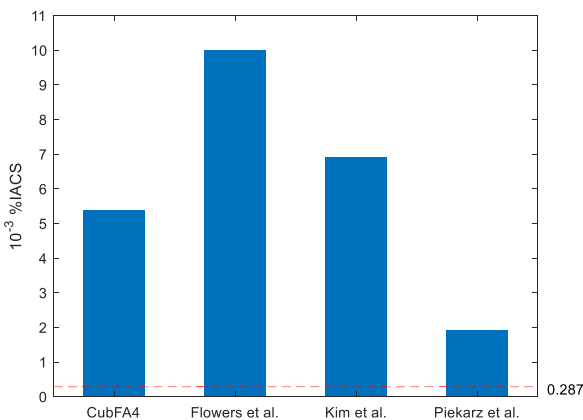
**Fig. 18** Cross-sections **a** sub-part 1 **(b)** sub-part 2 **c** sub-part 3 of a cuboid printed with parameter set FB4

Table 7 Results of complex coil printing with filament A

Coils	Name	Printing parameter	Success	Reason of failure
	CoilFA1a	FA4	No success due to incomplete print	Extruded material is not dimensionally stable
	CoilFA1b	FA4	No success due to incomplete print	Extruded material is not dimensionally stable
	CoilFA2	FA4	No success due to incomplete print	Extruded material is not dimensionally stable
	CoilFA3	FA4	No success due to incomplete print	Extruded material is not dimensionally stable

The fully printed coils are heat treated, but decompose during this thermal post processing. Big pores resulting from debinding, are assumed to be the reason.

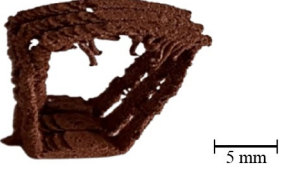
**Fig. 19** Comparison of the measured electrical conductivity of the filament A with similar values of the literature

5 Discussion

In Fig. 19, the measured electrical conductivity of the filament A is compared with previously published values for this filament. All results are set in relation to the manufacturer's recommendation [35, 36]. The electrical conductivity of all filament A values, both from the literature or obtained in the measurements conducted in this study, are above the manufacturer information which states a conductivity of $0.29 \cdot 10^{-3} \% \text{ IACS}$ ($5.94 \cdot 10^{-3} \Omega \text{cm}$). All published results are in the same order of magnitude of $10^{-3} \% \text{ IACS}$ ($1.72 \cdot 10^{-3} \Omega \text{cm}$). The results of Piekarz et al. [21] are lower than the measured electrical conductivities. The remaining results of Kim et al. [18] and Flowers et al. [14] are slightly more conductive.

In-plane measurements of the electrical conductivity were performed in this study. But in principle, there is a difference between the in-plane or out-of-plane measurement of the electrical conductivity. According to the manufacturer information of filament A, the electrical

Table 8 Results of complex coil printing with filament B

Coils	Name	Printing parameter	Success	Reason of failure
	CoilFB1a	FB4 with print bed temperature of 70 °C	No success due to defects in windings	Adhesion of the windings to the print bed is not successfully due to the raft
	CoilFB1b	FB4 with print bed temperature of 70 °C	Success	–
	CoilFB2	FB4 with print bed temperature of 70 °C	No success due to incomplete print	Coil detached from the print bed during printing
	CoilFB3a	FB4 with print bed temperature of 70 °C	Success	–
	CoilFB3b	FB4 with print bed temperature of 70 °C	No success due to incomplete print	Filament is torn during feeding
	CoilFB3c	FB4 with print bed temperature of 70 °C	Success	–

conductivity of in-plane measurement (horizontal traces) is about $0.14 \cdot 10^{-3}$ % IACS ($0.012 \Omega \text{cm}$) in comparison to out-of-plane measurement (vertical tower) with $0.21 \cdot 10^{-4}$ % IACS ($0.085 \Omega \text{cm}$) [40]. In this study, an in-plane measurement of the electrical conductivity is performed. Piekarz et al. [21] Kim et al. [18] and Flowers et al. [14] also used in-plane measurement to determine the electrical conductivity. This could be the reason for the higher electrical conductivity compared to the manufacturer

information, since there is no information if they performed an in-plane or out-of-plane measurement.

The electrical conductivity of filament B printed with two different parameter sets and measured after the debinding and sintering process is illustrated in Fig. 20. There is little difference in the conductivity results of the two parameter sets FB2 and FB4. Overall, the conductivity of around 45 % IACS ($3.77 \cdot 10^{-6} \Omega \text{cm}$) is decent, but far from the targeted conductivity for electromagnetic space components of 100 % IACS ($1.72 \cdot 10^{-6} \Omega \text{cm}$).

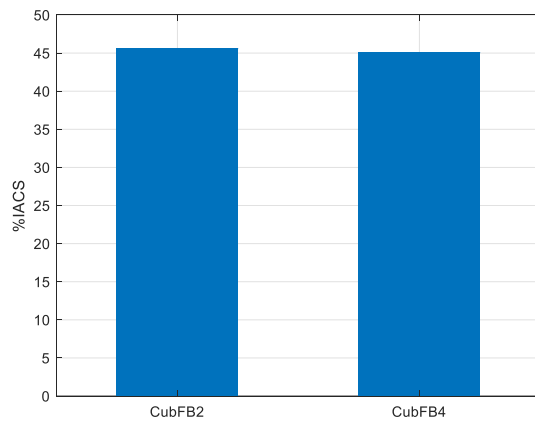


Fig. 20 Comparison of the electrical conductivity of the filament B with two different parameter sets

One possibility to increase the electrical conductivity could be a hot isostatic pressing (HIP) of the cuboids of filament B to reduce the porosity of the printed parts.

The coils cannot be printed with filament A in any of the investigated orientations. The main problem is that the printed component is not dimensionally stable. As the printed material is too soft, complex geometries consisting of overhangs or filigree structures cannot be printed using the investigated parameter sets. Filament A was initially developed by Flowers et al. as coating material for antennas [14]. For the coating application, it is not necessary for filament A to be dimensionally stable and suitable for complex structures. The study results presented in this paper suggest that filament A is not suitable for printing complex geometries, such as the coil.

Filament B can be used to print coil geometries. However, the quality of the printed coils has to be enhanced through further adjustments of the FFF process. In the presented study, the coils failed during debinding and sintering. Thus, the heat treatment of complex and filigree structures made from filament B has to be adapted in the future.

Since meander was used as printing strategy, one possibility to improve the printing results is to use the contour printing strategy instead. This reduces the directional changes of the extruder, which is the assumed reason for the wavy pattern detected on cubes printed with filament A, and the overall print result can be improved, especially for filament A.

6 Conclusion

The presented study demonstrates the manufacturability of a complex coil geometry by FFF processing of a conductive copper filament. The electrical conductivity of material produced from two different filaments was measured via the four-wire method. The filament that

produces material that is electrically conductive in the as-built state reaches an electrical conductivity in the range of 10^{-3} % IACS ($1.72 \cdot 10^{-3} \Omega\text{cm}$). The filament that produces material that is electrically conductive only after a subsequent heat treatment process of debinding and sintering reaches an electrical conductivity around 45 % IACS ($3.77 \cdot 10^{-6} \Omega\text{cm}$).

Especially the latter results are promising with respect to future applications of conductive copper filaments for electromagnetic space components. FFF is beneficial compared to other AM processes, which use powder feedstock, with respect to feedstock handling and production costs.

Further investigations will have to be performed to improve the material density, heat treatment process, and thus electrical conductivity.

Acknowledgements The present work was performed in the frame of ZARM Technik AG's project Additive Manufacturing of Pure Copper Electromagnetic Coils, funded by the European Space Agency (ESA Contract No. 4000133077/20/NL/AR/idb), under the supervision of Prof. Dr. Antonio García Marín.

Funding Open Access funding enabled and organized by Projekt DEAL.

Declarations

Conflict of interest The authors declare that they have no conflict of interests.

Open Access This article is licensed under a Creative Commons Attribution 4.0 International License, which permits use, sharing, adaptation, distribution and reproduction in any medium or format, as long as you give appropriate credit to the original author(s) and the source, provide a link to the Creative Commons licence, and indicate if changes were made. The images or other third party material in this article are included in the article's Creative Commons licence, unless indicated otherwise in a credit line to the material. If material is not included in the article's Creative Commons licence and your intended use is not permitted by statutory regulation or exceeds the permitted use, you will need to obtain permission directly from the copyright holder. To view a copy of this licence, visit <http://creativecommons.org/licenses/by/4.0/>.

References

1. Gradl, P. R. et al.: "Progress in Additively Manufactured Copper-Alloy GRCop-84, GRCop-42, and Bimetallic Combustion Chambers for Liquid Rocket Engines," in 70th International Astronautical Congress (IAC), pp. 1-14. Washington D.C., USA (2019)
2. Gradl, P. R. et al.: "Development and Hot-fire Testing of Additively Manufactured Copper Combustion Chambers for Liquid Rocket Engine Applications," in 53rd AIAA/SAE/ASEE Joint Propulsion Conference 2017. Atlanta GA, USA (2017)
3. Gradl, P. R. et al.: "GRCop-42 Development and Hot-fire Testing Using Additive Manufacturing Powder Bed Fusion for Channel-cooled Combustion Chambers," in 55th AIAA/SAE/ASEE Joint Propulsion Conference 2019. Indianapolis IN, USA (2019)
4. Gradl, P. R. et al.: "Additive Manufacturing and Hot-fire Testing of Bimetallic GRCop-84 and C-18150 Channel Cooled Combustion Chambers Using Powder Bed Fusion and Inconel 625 Hybrid

- Directed Energy Deposition,” in 55th AIAA/SAE/ASEE Joint Propulsion Conference 2019. Indianapolis IN, USA (2019)
5. Seltzman, H., Wukitch, S. J.: “Nuclear response of additive manufactured GRCop-84 copper for use in Lower hybrid launchers in a fusion environment,” *Fusion Engineering and Design* **159**, 111726 (2020)
 6. Seltzman, H., Wukitch S. J.: “Surface roughness and finishing techniques in selective laser melted GRCop-84 copper for an additive manufactured lower hybrid current drive launcher,” *Fusion Engineering and Design* **160**, 111801 (2020)
 7. Seltzman, H., Wukitch, S.J.: Brazing, laser, and electron-beam welding of additively manufactured GRCop-84 copper for phased array lower hybrid launchers. *IEEE Trans. Plasma Sci.* **48**(6), 1579–1584 (2020)
 8. Gradl, P. R., Mireles, O. R., Andrews, N.: “Introduction to Additive Manufacturing for Propulsion and Energy Systems,” *AIAA Propulsion and Energy Forum* 2021, Virtual. (2021)
 9. Sau’de, N., et al.: Additive manufacturing of copper-ABS filament by fused deposition modeling (FDM). *J. Mech. Eng.* **5**(4), 23–32 (2018)
 10. Saroia, J., Wang, Y., Lei M. J.: “Experimental study of mechanical, electrical and thermal properties for 3D-printed copper nanoparticles/PLA matrix polymer composite,” in *CIE48 Proceedings*, pp. 183–193. The University of Auckland, Auckland, New Zealand (2018)
 11. Nabipour, M., Akhoundi, B., Saed, A.B.: Manufacturing of polymer/metal compo-sites by fused deposition modeling process with polyethylene. *J. Appl. Polym. Sci.* **137**, 2 (2020)
 12. Podsiadly, B. et al: Electrically conductive acrylonitrile butadiene styrene (ABS)/copper composite filament for Fused Deposition Modeling. In: *Proceedings of SPIE 0277-786X*, V. 10808, Photonics Applications in Astronomy, Communications, Industry, and High-Energy Physics Experiments 2018. Wilga, Poland (2018)
 13. Vu, M.C. et al.: 3D printing of copper particles and poly(methyl methacrylate) beads containing poly(lactic acid) composites for enhancing thermomechanical properties. *J. Appl. Polym. Sci.* **138**, 5 (2021)
 14. Flowers, P.F., et al.: 3D printing electronic components and circuits with conductive thermoplastic filament. *Addit. Manuf.* **18**, 156–163 (2017)
 15. Cardenas, J. A. et al.: “Flash ablation metallization of conductive thermoplastics,” *Addit. Manuf.* **36**, 101409 (2020)
 16. Colella, R., et al.: Electromagnetic Analysis and Performance Comparison of Fully 3D-printed Antennas. In: *2019 Photonics & Electromagnetics Research Symposium*, pp. 964–970. Spring (PIERS-Spring), Rome, Italy (2019)
 17. Colella, R., et al.: Fully 3D-Printed RFID Tags based on Printable Metallic Filament: Performance Comparison with other Fabrication Techniques. In: *2019 IEEE-APS Topical Conference on Antennas and Propagation in Wireless Communications (APWC)*, pp. 253–257. Granada, Spain (2019)
 18. Kim, M.J., et al.: One-step electrodeposition of copper on conductive 3D printed objects. *Addit. Manuf.* **27**, 318–326 (2019)
 19. Mitra, D., et al.: On the Crosstalks between a Pair of Transmission Lines in the Presence of a 3D Printed Electrifi Trace. In: *2020 International Applied Computational Electromagnetics Society Symposium (ACES)*, pp. 1–2. Monterey CA, USA (2020)
 20. Mitra, D., et al.: On the Design of An Improved Model of Additively Manufactured Microstrip Transmission Lines for Radio Frequency Applications. In: *2019 IEEE International Conference on Electro In-formation Technology (EIT)*, pp. 182–184. Brookings SD, USA (2019)
 21. Piekarz et al., “Suspended Microstrip Low-Pass Filter Realized Using FDM Type 3D Printing with Conductive Copper-Based Filament,” in *2018 IEEE 68th Electronic Components and Technology Conference (ECTC)*, pp.2470-2476. San Diego CA, USA (2018)
 22. Watschke, H., Hilbig, K., Vietor, T.: Design and characterization of electrically conductive structures additively manufactured by material extrusion. *Appl. Sci.* **9**(4), 1–25 (2019)
 23. Striker, R.: “On the Manufacturing Process of a Single-Step Fully 3D Printed Conformal Patch Antenna,” in *2020 IEEE International Conference on Electro Information Technology (EIT)*, pp. 288–292. Chicago IL, USA (2020)
 24. Ebrahimi, N.D., Ju, Y.S.: Thermal conductivity of sintered copper samples pre-pared using 3D printing-compatible polymer composite filaments. *Addit. Manuf.* **24**, 479–485 (2018)
 25. Alafaghani, A.Q., Ablat, M.A.: Design consideration for additive manufacturing: Fused deposition modelling. *OJAppS* **07**(06), 291–318 (2017)
 26. Eguren, J.A., Esnaola, A., Unzueta, G.: Modelling of an additive 3D-printing pro-cess based on design of experiments methodology. *QIP Journal* **24**(1), 128 (2020)
 27. Griffiths, C.A., Howarth, J., Almeida-Rowbotham, G.D., Rees, A.: “A design of experiments approach to optimise tensile and notched bending properties of fused deposition modelling parts,” *Proceedings of the Institution of Mechanical Engineers. Part B: J. Eng. Manuf.* **230**(8), 1502–1512 (2016)
 28. Han, S., Xiao, Y., Qi, T., Li, Z., Zeng, Q.: Design and analysis of fused deposition modeling 3D printer nozzle for color mixing. *Adv. Mater. Sci. Eng.* **2017**, 1–12 (2017)
 29. Nidagundi, V.B., Keshavamurthy, R., Prakash, C.P.S.: Studies on parametric optimization for fused deposition modelling process. *Mater. Today: Proc* **2**(4–5), 1691–1699 (2015)
 30. Durão, L.F.C.S., Barkoczy, R., Zancul, E., Lee Ho, L., Bonnard, R.: Optimizing ad-ditive manufacturing parameters for the fused deposition modeling technology using a design of experiments. *Prog. Addit. Manuf.* **4**(3), 291–313 (2019)
 31. Kim, M.K., Lee, I.H., Kim, H.-C.: Effect of fabrication parameters on surface roughness of FDM parts. *Int. J. Precis. Eng. Manuf.* **19**(1), 137–142 (2018)
 32. Yang, J., Liu, Y.: Energy, time and material consumption modeling for fused deposition modelling process. *Procedia CIRP* **90**, 510–515 (2020)
 33. Cuan-Urquizo, E., Barocio, E., Tejada-Ortigoza, V., Pipes, R.B., Rodriguez, C.A., Roman-Flores, A.: Characterization of the mechanical properties of FFF structures and materials: A review on the experimental, computational and theoretical approaches. *Materials (Basel, Switzerland)* **12**(6), 1–25 (2019)
 34. Ćwikła, G., Grabowik, C., Kalinowski, K., Paprocka, I., Ociepka, P.: The influence of printing parameters on selected mechanical properties of FDM/FFF 3D-printed parts. *IOP Conf. Ser: Mater. Sci. Eng* **227**, 012033 (2017)
 35. Multi3D, Electrifi Conductive Filament | Multi3D. <https://www.multi3dllc.com/product/electrifi/>. Accessed 5 Feb 2021
 36. Multi3D, FAQs | Multi3D. <https://www.multi3dllc.com/faqs/>. Accessed 5 Feb 2021
 37. Filamet copper | Filament2Print. https://filament2print.com/gb/metallic/1029-filamet-copper.html#/260-format-spool_500_g/242-diameter-285_mm. Accessed 5 Feb 2021
 38. Metal Filament to Pure Metal 3D Print., How to 3D Print Metal—Metal Filament to Pure Metal 3D Print. <https://www.thevirtualfoundry.com/help/>. Accessed 5 Feb 2021
 39. The Virtual Foundry, Copper Filamet™. <https://shop.thevirtualfoundry.com/products/copper-filamet?variant=12351243288659>. Accessed 5 Feb 2021
 40. Multi3D, Electrifi Conductive Filament. <https://www.multi3dllc.com/faqs/>. Accessed 5 Feb 2021

Publisher's Note Springer Nature remains neutral with regard to jurisdictional claims in published maps and institutional affiliations.